UNRAVELLING THE RELATIVE IMPORTANCE OF IMPACT FORCES IN DEBRIS FLOWS OF DIFFERENT COMPOSITION

MSc. Thesis Earth Surface and Water

Ika Prinadiastari

Student Number: 6139981

Email: i.ikaprinadiastari@students.uu.nl

First supervisor: Tjalling De Haas

Second supervisor: Steven de Jong

28-02-2020

ABSTRACT

Debris flows are mixtures of water and sediment that flow rapidly down a slope due to gravity force (Iverson, 1997; Takahashi, 2014). They are destructive to property and often fatal, a single event potentially killing thousands of people (Iverson, 1997 and 2011; Haas and Woerkom, 2016). The catastrophe is worsened when the volume of debris flow increases by bed entrainment caused by the interaction between flowing particles and bed particles (Takahashi, 1981; Pierson et al., 1990; Haas and Woerkom, 2016). Bed entrainment may result from impact forces and basal-shear forces and are mainly driven by the debris flow composition. However, it has long been unclear whether impact or basal-shear forces bear more responsibility in the erosion process, or it is a combination of both forces. This study shows that impact forces play a critical role in the occurrence of debris flows, and thereby in the erosion of bed material. Geophone capable of quantifying impact forces, and load cell capable of measuring flow weight in dry granular flows (representing debris flows) were used on laboratory-scale simulations. Impact forces were strongly controlled by debris flow composition (i.e. grain-size distribution) and moderately by flow properties (i.e. flow depth, flow weight, flow velocity). Thus, impact forces significantly affect debris-flow erosion, mainly by progressive scour rather than mass failure. Impact forces possibly result in bed entrainment, which is related to increasing debris-flow volume. A better understanding of how the debris-flow volume increases will help minimise the negative impacts of debris flows as well as strengthen hazard mitigation strategies.

TABLE OF CONTENT

1. INTRODUCTION

Debris flows are a mixture of water and coarse-to fine-grained sediment. It is a mass movement down a slope due to gravity force and mainly occurs in mountainous areas (Iverson, 1997 and 2011; McArdell et al., 2007; Coe et al., 2008). Debris flows could kill thousands of people and destroy property, especially in densely-populated locations (Iverson, 1997 and 2011; Haas and Woerkom, 2016), and the catastrophe worsens if the debris-flow volume increases and exceeds the channel capacity, or overwhelms the infrastructural capacity built into the channel (Haas and Woerkom, 2016). A better understanding of how the debris-flow volume increases during its motion is vital to minimise the negative impacts of debris flows as well as to strengthen the hazard mitigation strategies, particularly as landscape over-exploitation and climate instability increase (Iverson et al., 2011).

One dominant process that increases debris-flow volume is by entraining the bed material during movement through the channel due to an interaction between particles within debris flows and the bed material (Takahashi, 1981; Pierson et al., 1990; Haas and Woerkom, 2016). Bed entrainment may result from impact forces and basal-shear forces. Impact forces erode the bed material by material colliding with the bed surface, while basal-shear forces erode the bed material by material sliding along the bed surface.

The debris flow composition mainly drives impact forces and basal-shear forces in bed entrainment. However, it is still unclear if one type of forces contributes more to erosion by the debris flow, or it is a combination of both forces. The grain size distribution and pore-fluid content determine the debris flow composition (McArdell et al., 1997; Haas and Woerkom, 2016) and also influence the cohesion, friction, and collision behaviour of its particles (Iverson, 1997).

Many recent laboratory experiments have focused on the effect of debris flow composition, primarily on the mechanism of erosion and deposition, and the debris-flow fan (e.g. De Haas et al., 2015; Haas and Woerkom, 2016). Haas and Woerkom (2016) developed an experimental flume to investigate the effect of debris flow composition on the amount and spatial pattern of bed scour. In assessing the relationship between debris flow composition and debris flow size, they found that the grain size distribution was critical in determining the relative effect of grain collisional and basal-shear stress to the bed surface. Moreover, debris flow composition also defined debris flow behaviour (i.e. collisional, frictional or viscous parameter). The study by Haas and Woerkom (2016) indicated that impact forces might predominate over basal-shear forces when the flow thickness of debris flows increased linearly with depth to balance the gravitational stress (Iverson, 1997).

Another study by Hsu and Dietrich (2014) utilised a rotating drum with a load cell. In those experiments, basal normal forces were strongly controlled by flow properties (i.e. grain-size distribution, flow velocity, nature of the interstitial fluid). A similar rotating drum experiment by Yohannes et al. (2012) investigated the influence of grain-size on contact forces associated with particle-bed impacts. The authors found that particle size dependence supported the proposed bedrock incision model. Cui et al. (2015) carried out a flume experiment with the load cell to measure the impact forces of viscous debris flows. The results indicated that large grains were prone to concentrate at the surface and middle part of the flow at the flow front. Also, the impact frequency increased with rising flow depth, notably in the coarser grains.

Despite many studies have investigated debris-flow erosion, mainly with the application of load cell, there has been relatively limited study on the relative importance of impact forces in debris flows, specifically using a geophone on a laboratory-scale. Rickenmann et al. (2012) compared a

geophone and an automated bucket sampler for measuring sediment transport at the Erlenbach stream. The results showed a linear relationship between impulses counted from the geophone and bedload mass passing over the sensors from the automated basket sampler. It demonstrated that the geophone was capable of measuring sediment transport in real-time.

This study aims to quantify impact forces in debris flows of different composition, and thus, unravel how impact forces affect debris-flow erosion. This study implements an expanded channel flume based on flume experiment by Haas and Woerkom (2016) and incorporates a geophone and load cell. A larger flume may able to reproduce the natural field-scale debris flows, while the implementation of geophone and load cell may help to improve their laboratory-scale use for quantifying impact forces.

This thesis includes an introduction as the first chapter, followed by a literature review defining and classifying debris flows. Then, the current understanding of bed entrainment is presented, followed by the erosion mechanism, focusing on the effect of debris flow composition and dry granular flows. Recent experimental methods, implementation of laboratory experiments, and measurement devices in quantifying impact forces are also discussed. The research questions and hypotheses are provided and followed by the materials and methods used in this study. Thus, the impact forces in debris flows of different composition and how they affect debris-flow erosion are analysed. The last chapter is focused on the results, discussion, and conclusion.

2. LITERATURE REVIEW

2.1. Debris flows definition and classification

Debris flows are poorly-sorted sediment mixtures, saturated with water, then flows down the channel because of solid and fluid forces that directly influences its motion and demonstrate a unique destructive power (Iverson, 1997; Takahashi, 2014). Solid forces dominate the physics of avalanches, which typically have a total sediment concentration exceeding 50% of its volume (Iverson, 1997 and 2011). In contrast, fluid forces control the physics of floods. The combination of solid forces and fluid forces may generate debris flows to travel a longer distance and inundate a larger area (Iverson, 1997).

Both solid and fluid forces play vital roles in the occurrence of debris flows. In addition, they also define the debris flows in terms of the sediment concentration, grain size distributions, flow front speeds, shear strength, and shear rates (e.g. Beverage and Culbertson, 1964; Varnes, 1978; Pierson and Costa, 1987). Interaction of solid and fluid forces supports a broader interpretation, classifying events such as debris slides, debris torrents, debris floods, mudflows, mudslides, mud-spates, hyper-concentrated flows, and lahars as debris flows (Johnson, 1984). Iverson (1997) found that the variable nomenclature reflects the diverse origins, compositions and appearance of debris flows, from quiescently streaming, sand-rich slurries to tumultuous surges of boulders and mud.

Takahashi (2014) classified debris flows occurrence in two stages: 1) quasi-static debris flows during the initiation and deposition phase; 2) dynamic debris flows during the motion phase. Thus, there are three types of dynamic debris flows based on their appearance (*Figure 2.1*): 1) when grain collision stress dominates, the debris flow becomes the stony-type in which the largest stones accumulate in the front part, followed by mudflow in the tail; 2) when turbulent mixing stress dominates, it becomes the turbulent-muddy-type which is mainly comprised of fine ash (e.g. pyroclastic flow) and can also contain large boulders, with a turbulent flow, and solid concentration is 35-40% of the total volume; and 3) when viscous stress dominates, it becomes the viscous-type, an intermittent bore-like flow with many surges emitted repeatedly, resulting in a flat riverbed which reaches a deposition equilibrium stage. Thus, continuous turbulent debris flows appear and is followed by the hyper-concentrated flood flows, which erodes the smoothened bed.

Figure 2.1 Three types of dynamic debris flows by Takahashi (2014): (a) The stony-type debris flows (Kamikamihorizawa); (b) The turbulent-muddy debris flows (Nojiri River, Sakurajima); (c) The viscous-type debris flows (Jiangjia).

The asymptotic configuration of debris flows is shown in *Figure 2.2* in which the flow front is primarily filled with coarse-grained material, while the tail fill is more finer-grained (Iverson, 1997). Massive material accumulates at the flow front due to lack of gravity force and boundary to force the material submerged while agitated. It can be incorporated and retained there if the flow acquires the material in transit, and can migrate to the head by preferential transport (Iverson, 1997).

Furthermore, the flow velocity at the flow front accelerates as long as it travels, while flow velocity at the flow body accelerates less. The different flow velocities between flow front and flow body make the flow extend in length and reduce flow depth, which linearly increases the time and travel distance. Then, the debris flows decelerate and start to deposit and create a debris flow alluvial fan (Iverson, 1997). The flow velocity becomes larger if the higher the flow depth and the steeper the channel gradient. However, it also depends on the solid concentration, in which the denser the consolidation, the slower the flow velocity (Takahashi, 2014).

The solid and fluid fractions determining the type of debris flows and also influencing the cohesion, friction, and collision behaviour of its particles, as those elements may transfer significant momentum simultaneously (Iverson, 1997). Moreover, the debris flow composition mainly drives impact forces and basal-shear forces in bed entrainment, which defines the specific forces that are more dominant during the initiation and motion phase of debris flows. The motion phase is a critical phase where the debris-flow volume may increase due to bed entrainment.

Based on Takahashi (2014), the impact forces likely dominate the flow in the stony-type debris flows due to a higher solid fraction than a fluid fraction. Therefore, the relative importance of impact forces in a different type of debris flows needs to be examined.

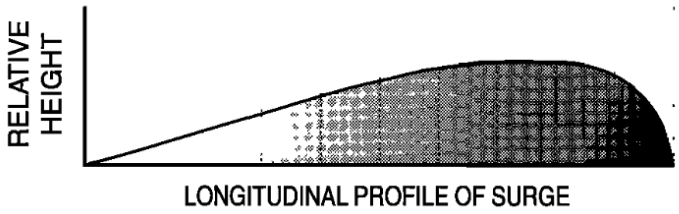

Figure 2.2 The longitudinal profile of debris flows (Iverson, 1997).

2.2. Debris flows initiation and development due to bed entrainment

2.2.1. Debris flows initiation

The occurrence of debris flows may result from the mobilisation of individual or numerous small failures that coalesce downstream (Iverson, 1997) and form the surface runoff, which is mainly occurred in the drainage basin, triggered by sufficient availability of material, high intensity and long duration of rainfall and steep slope (Coe et al., 2008; Kean et al., 2013). Failures on all scales, from single grains to enormous landslides, are generated from a combination of grain friction, grain collision, and viscous fluid flow (Mitchell, 1976; Iverson, 1997), changes in pore pressure distributions (Sharp and Nobles, 1953; Sitar et al., 1992; Iverson, 1997), and inertial forces (Iverson, 1997).

Takahashi (2014) illustrated the debris-flow initiation and development due to different bed slope (*Figure 2.3*). It begins when the surface water flow enters the channel upstream. In areas 1(a) and 1(b), the hydrodynamic forces erode the bed and mix with the surface water flow. Thus, when the flow reaches area 2, the seepage water saturates the bed. The upper part of bed later becomes unstable, and once again blends with the flow and moves downstream. In area 3, the flow is deposited or transferred downstream.

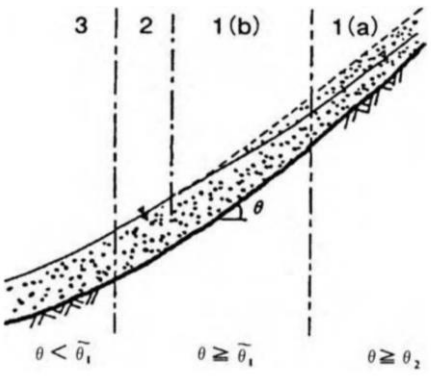

Figure 2.3 The debris-flow initiation and development due to different bed slope (Takahashi, 2014).

2.2.2. Bed entrainment

The debris-flow initiation and development may affect the bed entrainment mechanism wherein debris flows may grow severalfold by entraining bed material or eroding riverbank as they mix with the water and increase the volume, concentration, speed and runout of debris flows during its flow downslope (Pierson and Scott, 1985; Reid et al., 2011; Iverson et al., 2011). Haas and Woerkom (2016) discussed two known mechanisms of bed entrainment:

1) Entraining or incorporating bed sediments grain by grain occurs in the form of uniform lateral distribution and the upward decrease, driven by fluid dynamic forces (e.g. Takahashi, 2014).
2) En masse failure of parts of the bed occurs as localised failures of parts of the bed rather than massive failures over substantial portions of the bed, which is motivated by gravity force (e.g. Takahashi, 2014).

Channel deformation, steeper slope, and wetter bed sediment (Theule et al., 2015; Reid et al., 2011; Iverson et al., 2011) may trigger the debris flow entrainment mechanism. The combination of a relatively large amount of sediment and rapid flow velocity implies an increase in flow momentum (Haas and Woerkom, 2016; Reid et al., 2011; Iverson et al., 2011). This is because increasing pore pressure facilitates progressive scour of the bed, reducing basal friction and instigating positive feedback that causes flow velocity, mass and momentum to increase (Iverson et al., 2011).

When debris flows grow by the mass movement, the predominant process that occurred was an impact erosion, which happens when the debris avalanche material encounters the bed material, erodes the bed and generates a plowing bed. Then basal abrasion, which occurs when the avalanche materials slide parallel to the bed material (Lu et al., 2016).

Bed entrainment develops due to a mass transfer from flow materials to the bed material wherein impact forces and basal-shear forces act during this transfer process, then together with flow velocity, generates a flow momentum. Impact forces may dominate when the debris flow grows by entraining or incorporating of bed sediments grain by grain due to a sudden interaction between the flow particles with the bed material. Thus, a study needs to investigate how impact forces affect bed entrainment, specifically by the mechanism of entraining or incorporating bed sediments grain by grain.

2.3. Erosion mechanism and process

2.3.1. Debris flow composition

Debris flow composition controls a vital aspect in the dynamics of debris flow by affecting the occurrence of the forces during its movement (Iverson, 1997; McArdell et al., 2007), the type of the flow (Johnson, 1984; Iverson, 1997) and the cohesion, friction and collision behaviour of its particles (Iverson, 1997). Furthermore, the grain-size distribution and pore-fluid pressure also determine the debris flow composition. The grain-size distribution varies significantly from the coarse-grained to fine-grained, while the pore-fluid pressure, nearly incompressible with viscous liquid (composed of water with suspended silt and clay), may actively mediate intergranular friction and collisions (Iverson, 1997). In general, an increase in grain size will make scour depth even more extensive (Haas and Woerkom, 2016).

Debris flows consist of the flow front, which swells and carries large material and related items (i.e. downed trees, mangled bridges, or distressed automobiles; Iverson, 1997), and the tail, which contains more water and material with a smaller grain size than that in the front (Takahashi, 1981). On account of forces within the flow, the forces expected to be highest at the flow front, where the flow depth is largest and coarser sediment is concentrated (Haas and Woerkom, 2016; e.g. Berger et al., 2011). The majority of erosion is observed to take place during the passage of the flow front (Berger et al., 2011), because of the impact stresses of coarse particles recirculating at the flow front and the high basal-shear stress resulting from the relatively large flow depth at the flow front.

Flume experiment by De Haas et al. (2015) showed that the debris flow composition mainly affects the flow dynamics (e.g. flow velocity, flow depth), thus probably also their erosive potential. Furthermore, Haas and Woerkom (2016) discovered that the relative effect of grain collisional stress becomes more significant when debris-flow volume increases (e.g. flow depth). The erodibility increased when gravel fraction also increased, which may be related to the increase in grain collisional stress enhancing the total stress at the bed and thus erosion. In addition, the erodibility decreased when clay fraction increased in which may demonstrate a correlation between a decrease in grain collisional stress and an increase in viscous flow behaviour (e.g. Iverson, 1997). Another study by Hsu et al. (2008) indicated a strong dependence of erosion on particle diameter (e.g. debris flow composition) and a moderate dependence on the shear rate of the flow (e.g. particle collision with the bed).

Debris flow composition primarily encourages impact forces and basal-shear forces, thus affecting the debris-flow erosion. Therefore, the flume experiments are qualitatively applicable as shown by De Haas et al. (2015), and Haas and Woerkom (2016) to improve understanding of how debris flow composition drives the impact forces, and how it affects the debris-flow erosion.

2.3.2. Dry granular flows in representing debris flows

Debris flows are differentiated from dry granular flows by the pervasive, fluid-like deformation of the mobilised material (Moriguchi et al., 2009). Nevertheless, several experiments were performed on dry granular mixtures (Barbara and Alberto, 2006) and concluded to be capable of representing the debris flows mechanics (Takahashi, 1991; Egashira et al., 2001; Yamagishi et al., 2003). Both debris flows and dry granular flows can sustain shear stresses while remaining static; both can deform in a slow, tranquil mode characterized by enduring, frictional grain contacts;

and both can flow in a more rapid, agitated mode characterised by brief, inelastic grain collision (Iverson, 1997).

Moreover, dry granular flow regimes (*Figure 2.4*) can be divided into three types (Jiang et al., 2015; Takahasi, 1937; Savage, 1984): 1) rapid-dilute regime, in which instantaneous contact occurs among particles (collisional contacts) and causes higher mean velocity; 2) intermediate (granular liquid) regime, in which particles interact with collisional and frictional contacts with intermediate velocity; and 3) quasi-static regime, in which particles interact with each other through sustained contact (frictional contacts) at a lower mean velocity. Most geo-flows (i.e. rock avalanches, dry landslides, snow avalanches) are in the intermediate regime. The different regimes have different flow velocities, in which flow velocity difference caused the length of the sliding mass to increase and the depth to decrease (Jiang et al., 2015).

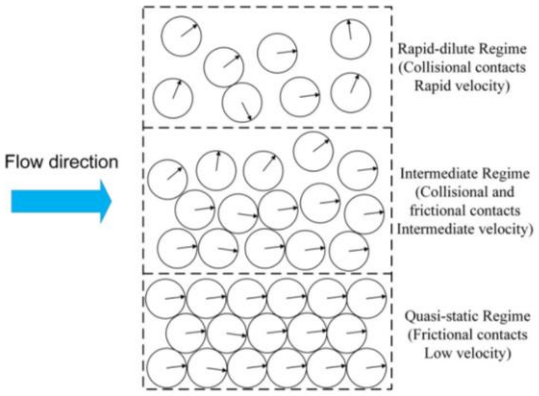

Figure 2.4 The differences between three dry granular flow regimes (illustrated by Jiang et al., 2015).

2.3.3. Quantification of impact forces

Debris flows are a highly concentrated mixture of coarse particle and water, and during its transport may result in forces due to 1) collision between coarse particles; 2) the macro turbulent mixing of the fluid body comprised of particles and slurry; 3) the enduring particle friction between particles when contained coarse particles are denser than a boundary value; 4) the deformation of interstitial fluid or the apparent viscous fluid consisting of the mixture of particles and slurry; 5) the interaction between particles and fluid resulting from the relative motion of the solid and fluid constituents (Takahashi, 2014).

Impact forces are inertial forces resulting from the collision between flow particles with the bed while proceeding downslope, thus eroding the bed material (Takahashi, 2014). Impact forces can be calculated based on the solid inertial normal stress (σ_i) which arise from inter-particle collisions, resulting in fluctuations of inertial particle impacts (Ogawa, 1978; Iverson and Vallance, 2001; Bagnold, 1954). The impact forces (σ_i) can be calculated with equation (1):

$$\sigma_i = v_s \rho_p {D_p}^2 \gamma^2 \quad (1)$$

Where v_s is volumetric solids concentration, ρ_p is particle density (kg m^{-3}), D_p is effective particle diameter (median grain-size in m) and γ is the shear rate (s^{-1}) which defined as (Iverson, 1997):

$$\gamma = \frac{\mu_s}{h} \quad (2)$$

Where μ_s is the flow surface velocity (m s^{-1}) and *h* is the flow depth (m). The shear approximation assumes a constant flow velocity for all experiments, even though in reality, the flow velocity

distribution generally deviates from linear debris flows (Kaitna et al., 2014; Haas and Woerkom, 2016).

Other forces may result from debris flow motion is the basal-shear forces which can be estimated with shear stress (τ in Pa) (Haas and Woerkom, 2016):

$$\tau = \rho g h \sin(\theta) \quad (3)$$

Where ρ is flow density (kg m^{-3}), g is the gravitational acceleration (m s^{-2}), h is the flow depth (m), and θ is slope angle (degree).

A rotating drum experiment by Hsu and Dietrich (2014) showed a consistent use of the solid inertial normal stress by Equation (1) to characterise bedrock lowering by impacting particles. Furthermore, it demonstrated that forceful impacts mainly occur at the flow front. The study used a load cell to quantify the total basal normal forces wherein the momentum transferred is equal to the force on the boundary integrated over time, also known as the impulse (I). Total impulse is described as the sum of mean force ($\bar{F}$), an average load on the boundary, and fluctuating forces (F't), a deviation from mean force ($\bar{F}$) which is caused by grain collisions, as shown in Equation (4) (Hsu and Dietrich, 2014):

$$I = \bar{F} \int dt + \int F'(t) \quad (4)$$

$$\text{Where } F'(t) = F(t) - \bar{F} \quad (5)$$

Equation (4) represents the momentum transferred by the quasi-static load, while Equation (5) by the dynamic collisions (Hsu and Dietrich, 2014). Debris-flow erosion is related more to the fluctuating forces than mean forces wherein the fluctuating forces are more dependent on flow properties (e.g. grain size distribution, flow velocity). The fluctuating forces are directly related to the incoming particle diameter because the size and density of the particle determine the mass for momentum transfer (Hsu and Dietrich, 2014).

2.3.4. Laboratory experiments

Numerous laboratory experiments such as miniaturised flume experiments (Cui et al., 2015; Armanini, 1997; Arattano and Franzi, 2003; Armanini et al., 2004, 2011; Zanuttigh and Lamberti, 2006; Huang et al., 2007) and rotating drum experiments (Hsu and Dietrich, 2014; Yohannes et al., 2012) have resulted in a better understanding of debris-flow erosion, particularly on the effect of debris flow composition (De Haas et al., 2015; Haas and Woerkom, 2016) and flow properties (i.e. grain-size distribution, flow velocity, interstitial fluid; Hsu and Dietrich, 2014; Yohannes et al., 2012).

Cui et al. (2015) carried out flume experiments with load cells to measure the impact forces of viscous debris flow and compared the experimental results with recorded field data. The study focused on the distribution of the impact forces at different depths and variations of the impact process over time, using wavelet analysis to separate the raw signals from the load cell to quantify the impact forces. The result indicated that large grains are prone to concentrate at the surface and middle part of the flow, at the flow front. Also, the impact frequency increased with rising flow depth, notably in the coarser grains. Therefore, it divided the impact process into three phases by analysing the variation of impacts signals and flow regimes: 1) sudden strong impact of the debris flow front when the peak impulse shape occurred; 2) continuous dynamic pressure of the body; and 3) slight static pressure of the tail (Cui et al., 2015).

Several experiments have indicated that the variance of the impact forces depends on the distributions of grains in the flow (Cui et al., 2015; Hubl et al., 2009). Therefore, further testing needs to measure the impact forces in debris flows of different composition. This can be accomplished by using flume experiment based on Haas and Woerkom (2016) with a larger channel flume dimension and application of measurement instruments to measure the impact forces. A larger dimension may able to reproduce the natural field-scale debris flows, while the implementation of the sensors may provide new insight of its utilisation on the laboratory-scale measurement of impact forces.

2.3.5. Measurement devices

The utilisation of measurement devices both in laboratory and field measurements have been used to gain a better understanding of debris flows. Hsu and Dietrich (2014) investigated the bed erosion of debris flow using a load cell in a rotating drum experiment. The study showed that the magnitude and shape of the fluctuating force from the load cell were strongly controlled by flow properties (i.e. grain-size distribution, flow velocity, nature of the interstitial fluid).

Further research using a load cell in a rotating drum was undertaken by Yohannes et al. (2012) that investigated the influence of grain-size on contact forces associated with the particle-bed impacts by comparing the experimental observations with the DEM (Discrete Element Method) simulation. They found that the normal stress along the boundary of a granular flow depends primarily on the distribution of mass along the boundary and is mostly unrelated to the particle size distribution. In contrast, the statistical measures of the contact forces (i.e. mean, standard deviation, maximum impact forces) were found to depend strongly on the mean particle size. The study supported the particle size dependence of a recently proposed bedrock incision model and suggested that the next testing steps for the model require the statistics of tremendous impact velocities.

Even though recent studies have shown that the application of the load cell was useful in investigating the debris-flow erosion, another potentially useful apparatus is the geophone, used worldwide in indirect field measurement of sediment transport in the natural stream (e.g. Rickenmann et al., 2012; Wyss et al., 2016). It works by converting ground flow velocity into voltage. The deviation between voltage, called the seismic wave, was recorded and thereby created a particular signal containing a broad spectrum of information (Krein et al., 2008; Wyss et al., 2016). Geophone results can be calibrated if there is a significant correlation between a registered signal frequency and a physical property (e.g. grain-size distribution) of the sediment transport (Wyss et al., 2016). However, the relation can vary for different field sites (Mizuyama et al., 2010a) and specific hydraulic conditions such as flow velocity (Rickenmann et al., 2014); grain size and shape (Rickenmann et al., 2014), sediment transport rate (Rickenmann et al., 2014) and bed roughness (Wyss et al., 2016a).

Rickenmann et al. (2012) discussed how geophone was able to measure the sediment transport at Erlenbach stream, Switzerland. The geophone sensors were mounted underneath the metal plates installed along the crest of the check dam and during the sediment transportation, the material slide, rolls or saltates over the plate. The plate transmits impact shocks of the inertial mass moving in a geophone sensor coil, and an electrical potential is produced. Whenever the voltage exceeds a threshold value, the shock recorded it as an impulse (Rickenmann et al., 2012). The investigation showed a linear relationship between impulses counted from the geophone

and bedload mass passing over the sensors from the automated basket sampler. It demonstrated that geophone is capable of measuring sediment transport.

McArdell et al. (2007) discussed the field measurement of normal and shear stresses and fluid pore pressure of debris flows using the result from an instrumented force plate in Ilgraben catchment, Switzerland. The instrumentation consisted of devices to measure front flow velocity (with geophone), flow depth (with laser distance-measuring device), normal and shear forces and fluid pressure (with load cell). The relation of flow depth and geophone signal, measured stresses and calculated bulk mass densities are shown in *Figure 2.5*. The results showed that pore-fluid pressures are present in debris flows and contribute to their unusual mobility. The study suggested a particle-collision-induced dynamic pore pressure effect. Also, the pore-fluid pressures are most likely present in a more rapidly sheared flows, which may not be necessary to explain the large pore pressure values.

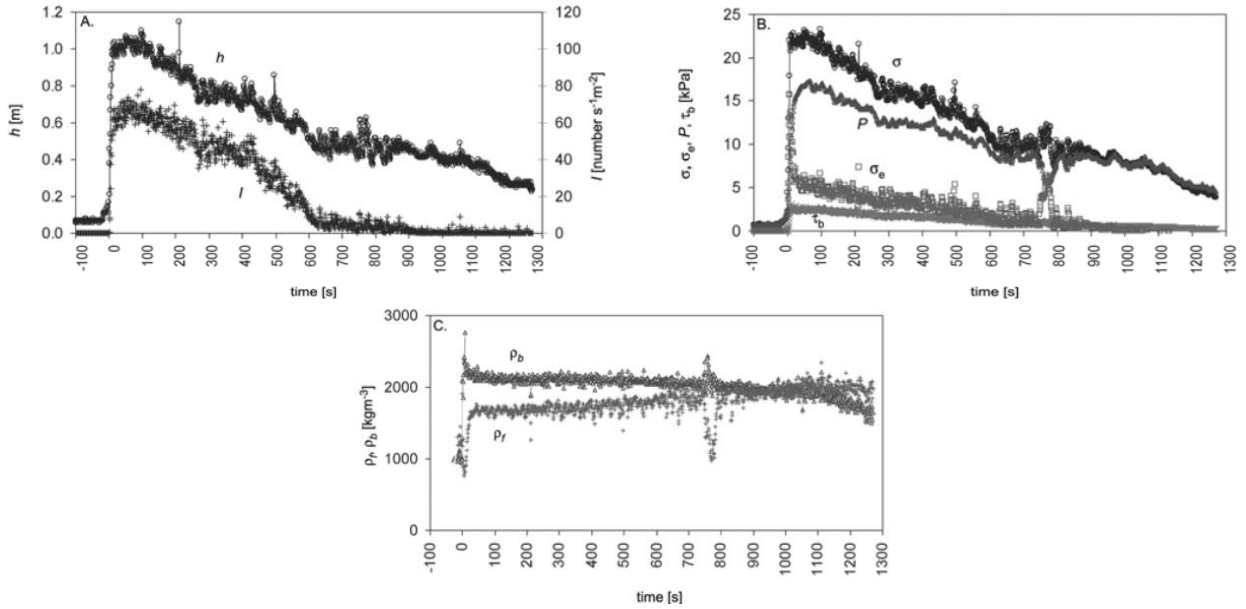

Figure 2.5 The results of geophone measurements in Ilgreban, Switzerland (McArdell et al., 2007).

Although the geophone has been widely used for field measurement and is capable of measuring sediment transport (Rickenmann et al., 2012) or front flow velocity (McArdell et al., 2007), its utilisation for the laboratory experiments is still limited. Thus, based on the flume experiment by Haas and Woerkom (2016) which implemented load cell to measure the forces within the debris flow, a geophone can be added in the flume to quantify the impact forces. The seismic wave performed by geophone and load cell can be statistically compared to investigate the sensors' capability in measuring impact forces.

2.4. Knowledge gap, research questions, and hypotheses

The debris flows may grow severalfold by entraining bed material or eroding riverbank, in which bed entrainment develops due to a mass transfer from flow materials to the bed material. The impact forces and basal-shear forces act during the mass transfer process, in which impact forces may dominate when the debris flow grows by entraining or incorporating bed sediments grain by grain due to a sudden interaction between the flow particles with the bed material. In addition, impact forces likely dominate the flow in the stony-type debris flows due to a higher

solid fraction than a fluid fraction (Takahashi, 2014). Debris flow composition primarily encourages impact forces and basal-shear forces, which affects debris-flow erosion.

Many studies have discovered a better understanding of debris-flow erosion, mainly by the application of load cells in the laboratory (Cui et al., 2015; Hsu and Dietrich, 2014; Yohannes et al., 2012). Moreover, geophone field measurements (Rickenmann et al., 2012; McArdell et al., 2007) proved its capability in measuring sediment transport or flow front velocity. Nevertheless, a limited study has been done on impact forces quantification, specifically by using a geophone on the laboratory-scale.

Therefore, further study using flume experiment based on Haas and Woerkom (2016) can be performed to unravel the relative importance of impact forces in debris flows of different composition, thus how impact forces affect debris-flow erosion. This study uses a larger dimension of channel flume, which may able to reproduce the natural field-scale debris flows, while the implementation of geophone and load cell may provide vital new insight into its utility on laboratory-scale quantification of impact forces.

The main question of this study is: How to quantify the impact forces in debris flows of different composition?

The sub-questions of this study are:

1) How similar are the geophone and load cell amplitude?
2) How does debris flow composition drives impact forces?
3) What is the correlation between impact forces and flow properties (i.e. flow depth, flow velocity)?
4) What is the relationship between impact forces and basal-shear forces?
5) How does impact forces affect debris-flow erosion?

This study will quantify impact forces in debris flows of different composition (i.e. grain-size distribution) at a variety of different slopes by using geophone and load cell. In addition, flow depth will be measured by using a laser distance measurement instrument at a certain point.

The hypotheses of this study are:

1) The geophone and load cell amplitudes show a similar characteristic that indicates the both sensors capability on the laboratory-scale simulations.
2) Impact forces are strongly controlled by debris flow composition (i.e. grain-size distribution) and moderately by flow properties.
3) Impact forces may dominate when the debris flow grows by entraining or incorporating of bed sediments grain by grain.
4) Erosion depends strongly on debris flow composition (i.e. grain-size distribution) and moderately on flow properties.

3. MATERIALS AND METHODS

The experimental setup was based on flume experiment by Haas and Woerkom (2016) with the added implementation of a larger channel flume and measurement devices (i.e. geophone, load cell, laser distance measurement instrument), while the methods were those referring to the quantification of impact forces discussed in the previous chapter. Note that the debris flows in this study are represented by dry granular flows which may able to reproduce more precise particle impacts on the bed.

3.1 Experimental design

3.1.1 Experimental equipment

The experimental equipment consisted of three parts, the first two of which were made from steel plates (*Figure 3.1*). The first part was a straight channel flume with a width of 0.3 m and a length of 5 m divided into two sections. The first section was a fixed-bed with a depth of 0.3 m and a length of 3 m in which the sensors were placed at the channel bed. The second section was an erodible-bed with a depth of 0.5 m and a length of 2 m, and the channel bed was filled with materials with a thickness of 0.05 m representing the natural bed surface. The flume length was sufficient to allow the front and body of the debris flows to reach an asymptotic configuration (constant shape of debris flows as shown in *Figure 2.2*) that flowed without deformation and to ensure the flow regimes were identical to natural field-scale debris flows while eroding the bed surface. The channel bed of the flume was covered with sandpaper with a thickness of 1 mm to represent the natural roughness of the bed surface. The outer sides of the flume were wrapped with a plywood board to dampen the noise to the sensors. The flume could be lifted until 35° to simulate the debris flows at a variety of different slopes.

The second part was the mixing tank with a side width of 1 m, fixed at the upstream end of the flume. The gate was installed at the front side of the tank, directly faced the flume channel and could be operated automatically. The third part was a plastic tray placed at the end of the flume to collect the material for re-utilization or discarded.

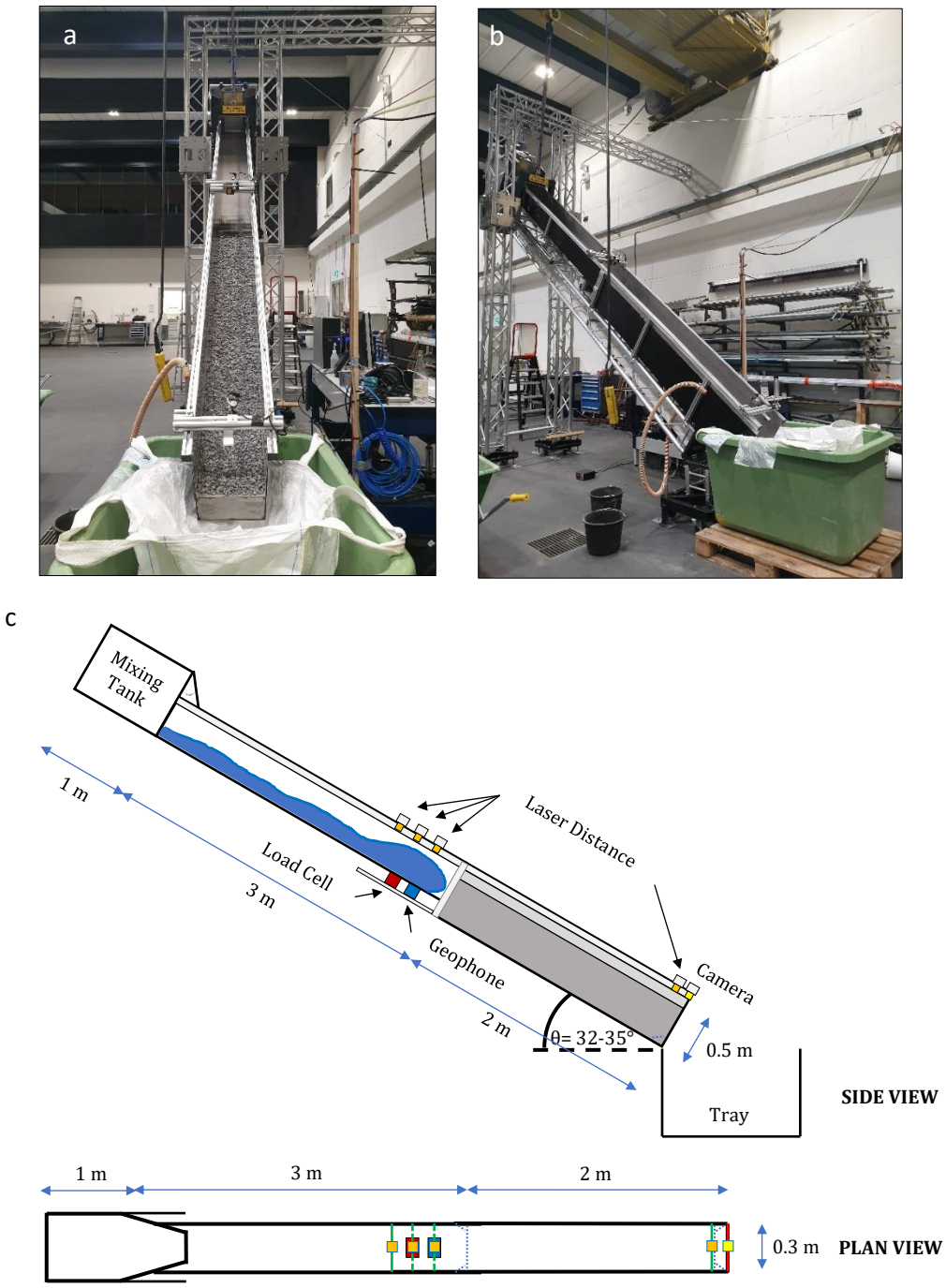

Figure 3.1 The debris-flow flume setup: (a) Front-view photograph; (b) Side-view photograph; (c) Schematic overview.

3.1.2 Experimental material

The dry granular flows and bed material were performed to replicate the erosion mechanism of natural field-scale debris flows. The flow composition was divided into three types: 1) coarse-grained flow with diameter d_{50} estimated at 9.76 mm; 2) fine-grained flow with diameter d_{50} estimated at 3.74 mm; 3) mixture flow of 50% coarse-grained and 50% fine-grained with diameter d_{50} estimated at 5.51 mm. The cumulative grain-size distribution and the friction diameter of the three flows are shown in *Figure 3.2*. The dry granular flows mass was 80 kg for

the first and second type, while the third type was 40 kg of coarse-grained and 40 kg of fine-grained. Before the materials were placed into the mixing tank, they were mixed by the concrete mixer to ensure homogeneity of the flow and to restraint materials segregation. The bed material was divided into two types: 1) coarse-grained bed with diameter d_{50} estimated at 9.76 mm; and 2) fine-grained bed, with diameter d_{50} estimated at 3.74 mm. The erodible-bed thickness was at 0.05 m, and the material mass was 60 kg for each type.

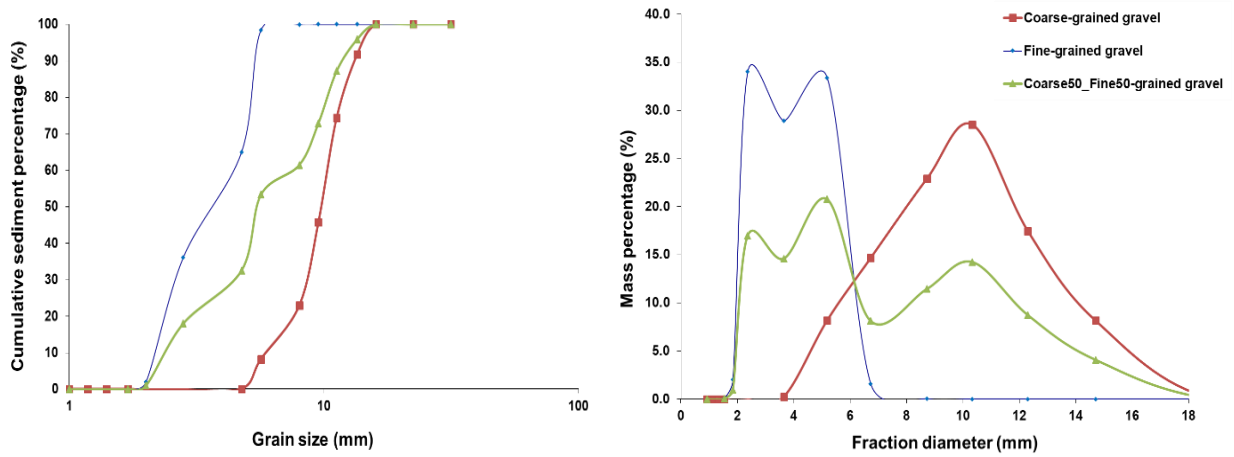

Figure 3.2 (a) The cumulative grain-size distribution and (b) the friction diameter of the three flows.

3.1.3 Measurements system

Flow depth, flow weight, and impact forces were recorded in real-time during the experiment within 30 seconds for each experiment. The impact forces detection system consisted of one geophone, one load cell, four laser distance measuring instruments, a data collection device and a computer (*Figure 3.3*). The geophone (Code: GS-20DX) measured the number and magnitude of particle impacts on the bed per unit of time, extracted from seismic waves generated by particle collision with the bed with a vertical and horizontal orientation, a 2.54 cm diameter and a sampling frequency of 10 Hz; the high frequency allowed detection of the transient impulse of the boulder impact forces. The load cell (Code: PW6D) quantified the bed pressure fluctuations with a maximum capacity of 3 kg. The geophone and load cell were mounted under the bottom part of the flume, which the sensors were connected to the channel bed surface in a rectangular area of 0.13 x 0.07 m^2 covered by sandpaper.

Two distance sensors (Code: OADM 20U2480/S14C) with a resolution of 0.015 to 0.67 mm were installed above the geophone and the load cell plate, while two distance sensors (Code: FADK 14U4470/S14/IO) with a resolution of 0.1 to 1 mm were placed at the upstream of the sensors and downstream of the channel, at the end of the flume. The instruments were used to record the flow depth of debris-avalanche before and after eroding the bed material. A digital camera (Go Pro Hero 6) was installed above the endpoint of the flume to record the mass movement process.

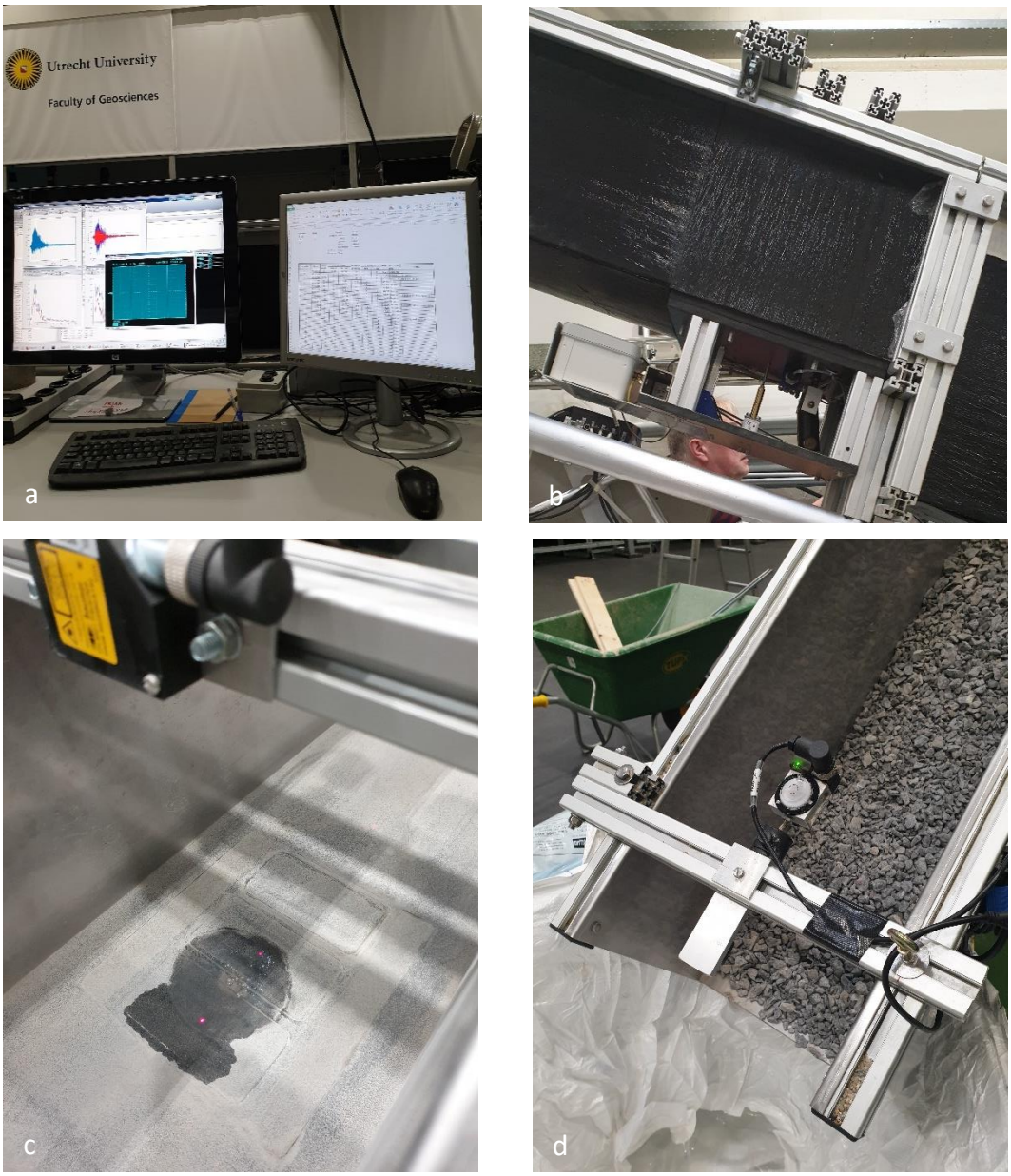

Figure 3.3 The impact forces measurement system: (a) A data collection device and a computer; (b) Geophone and load cell; (c) The sensors plate at the bed surface of flume; (d) A laser distance measuring instrument at the end of the flume.

3.2 Experiments and data analysis

3.2.1 Experiments process and flow properties

The measurement devices (i.e. geophone, load cell, laser distance measuring instrument) were calibrated before the experiments to examine whether the apparatus worked properly and to guarantee the accuracy of the acquired data, which results in a corrected equation. The equation was used to generate the real value of flow weight from the load cell and flow depth from the laser distance measuring instrument. The materials were placed inside the mixing tank at 90° to replicate the shape of debris-avalanche initiation. Once the gate was opened, the debris-avalanche was initiated, and the masses were transported into the flume, thus entraining the bed materials at the erodible-bed. The mass movement process was recorded in real-time by the geophone, the load cell and the laser distance measuring instruments. Three distance sensors

recorded the flow depth at the fixed-bed before entraining the bed material, while, the other recorded the flow depth after entraining the bed material at the erodible-bed. Additionally, a digital camera at the end of the flume was used to observed the moving process of the entire sliding masses. After the mass movement process finished, the amount of the bed materials at the erodible-bed was measured again, several photos were taken, and the recorded data was stored on a specific computer.

A total of 104 experiments were carried out with a different composition of dry granular flows and bed material, and channel slope varied from 32° to 35°. The measurement of bed material mass at the erodible-bed before and after the mass movement was to determine whether the mass movement resulted in erosion or deposition. To quantify the impact forces of debris flows and how they affect the debris-flow erosion, the experimental data used were only those that produced erosion.

Therefore, from 104 experimental data, a total of 59 experiments resulted in erosion during the mass movement process, as shown in Table 1 at Supplementary Material. Furthermore, to guarantee the experimental data used for analysis was reliable, there were eight samples not used in the analysis because most of the flow depth in those simulations resulted in a different asymptotic configuration of debris flows, in which two similar peak values at the flow regime emerged. Therefore, only 51 experimental data were used for further analysis.

The solid volumetric concentration (v_s) for the dry granular flows was estimated at one. Also, the flow properties were calculated to study the correlation of those parameters with impact forces during the bed entrainment process. The flow velocity was estimated by dividing the distance difference between the location of the sensor and the mixing tank gate, whereas the debris-avalanche started to flow, with the travel time of the flow measured from the start point to the sensor. This approximation created a constant value of flow velocity for all experiments.

3.2.2 Impact forces data acquisition and processing

The geophone recorded a seismic wave generated from the particle collision with the bed. The raw signals were denoised to obtain the real impacts signals by eliminating the random noise resulting from the measurement system and external disturbance. The denoising process involved converting the raw signals of the seismic wave into amplitudes, which represented the magnitude of particle impacts on the bed. The amplitude can be expressed as the fluctuating force, as shown in Equation (5) by reducing raw signals with a mean force (as an equilibrium point). The geophone amplitude had two orientations, vertical and horizontal which were denoised using the same method.

Meanwhile, the bed fluctuation pressure recorded from the load cell was converted into the flow weight, which also considered the channel slope as a correction factor and had been calibrated before the simulation. To compare the similarity of geophone and load cell, the load cell signal was also converted into amplitude, described as weight noise amplitude, using the same method as for the geophone. Before the load cell signal was converted into amplitude, it was corrected by reducing raw signals with a median value. The raw signal and amplitude of the geophone and the load cell are shown in *Figure 3.4*.

In this study, the impact forces were also calculated by using Equation (1), while the basal-shear forces were calculated by using Equation (3) and shown in Table 1 at Supplementary Material. The density value used for calculation of both forces was 2650 kg m^{-3} for gravel. The calculation resulted in relatively scattered results and a very high value for impact forces (*Figure 3.5a*). This

is likely due to the use of a constant value of flow velocity and neglects the effect of channel slope. In contrast, the calculation resulted in a more significant trend and formed a similar shape with debris flows asymptotic configuration for basal-shear forces (*Figure 3.5b*). Based on those considerations, in this study, the impact forces were quantified by using the geophone, while the basal-shear forces by using Equation (3).

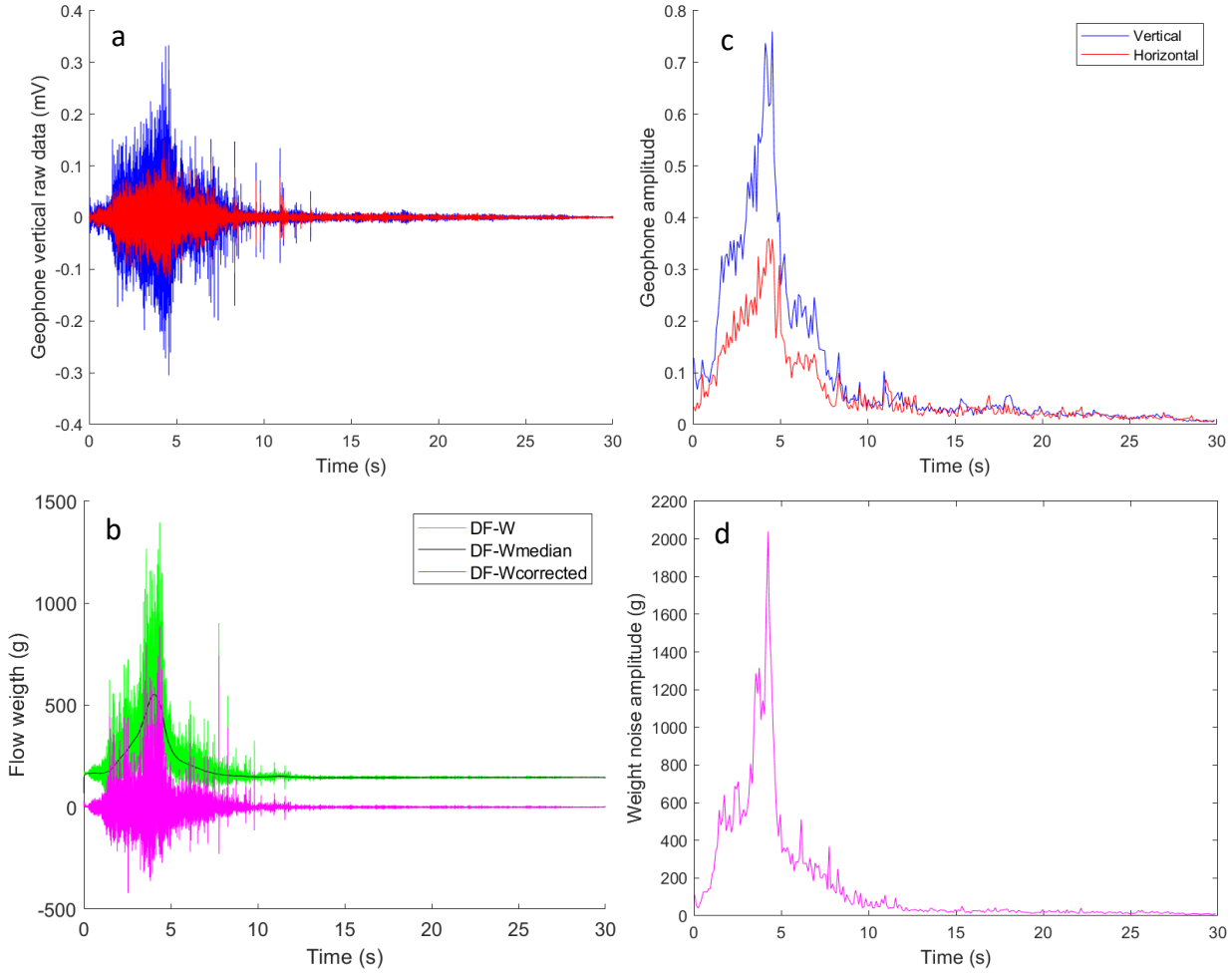

Figure 3.4 The raw signal of (a) Geophone; (b) Load cell; The amplitude of (c) Geophone; (d) Load cell. Examples from Test68 (coarse-grained flow).

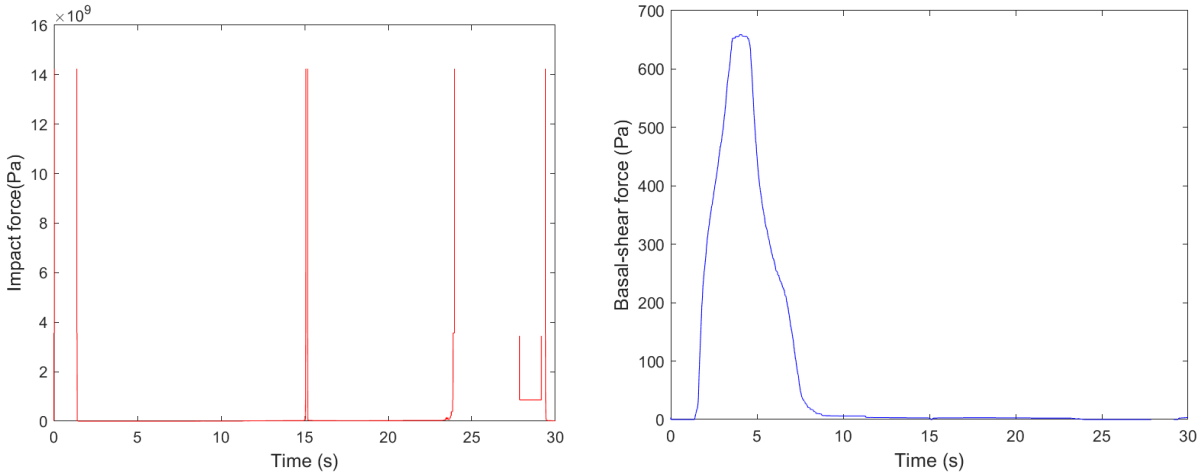

Figure 3.5 Calculation of (a) Impact force by using Equation (1) and (b) basal-shear forces by using Equation (3).

4. RESULTS

The flume experiments were able to represent debris flows mechanics, despite using dry granular flows and the differences in scale between the laboratory and natural debris flows events. In this study, for a comparison of debris flows with a different composition, Test68 described the coarse-grained flow, Test54 described the fine-grained flow, and Test99 described the mixture flow of coarse-grained and fine-grained, all of which had the same channel slope (33.2°). Note that the debris flows discussed in this and the next chapter are represented by dry granular flows and impact forces are described by geophone amplitude.

4.1 General description of flow behaviour

The experimental dry granular flows moved down the channel flume as a mass movement in a single surge, which represents an asymptotic configuration of debris flows. Flow depth increased rapidly at the flow front and decreased more gradually after the flow front has passed. Flow depths were highest at the flow front and decreased approaching the debris flow tail (*Figure 4.1*).

Flow depth did not directly increase at zero seconds because the sensor was not placed at the start point of the flow. Flow depth in the coarse-grained flow was the highest, while flow depth in the fine-grained flow was the lowest, but with a longer flow passage time.

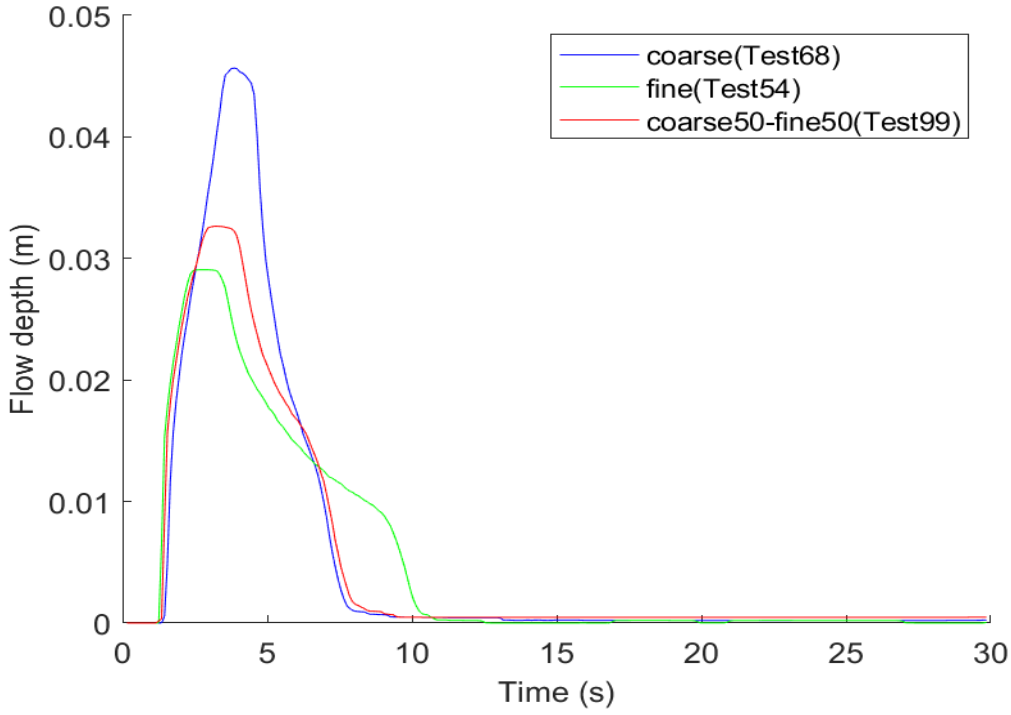

Figure 4.1 Characteristic development of flow depth over time; examples from Test68 (coarse-grained flow), Test54 (fine-grained flow), and Test99 (mixed flow). Maximum flow depth appears at the flow front, while lower flow depth emerges in the tail.

Flow depth increased with decreasing flow velocity for most flow compositions (*Figure 4.2b*). The coarse-grained flow had a relatively high flow depth with low flow velocity, while the finer-grained flow had a low flow depth with the high flow velocity. Although the variability was high, in general, flow velocity increased linearly with channel slope for all flow compositions (*Figure 4.2c*). For the same channel slope, flow velocity increased with decreasing grain-size. Flow depth decreased with the slope for most flow types, but there was considerable scatter in the trends, particularly in the fine-grained flow (*Figure 4.2a*). The flow depth of the coarse-grained flow

sharply decreased when the channel slope was larger than 33.5°, while in the finer-grained flow, there was a slight decrease in flow depth when the channel slope increased. For the same channel slope, flow depth increased with increasing grain-size.

In comparison with flow weight, it is very likely that flow depth scaled linearly with flow weight and showed the same behaviour as the relationship between flow depth and flow velocity. Flow velocity did not necessarily become faster at higher flow depth and steeper channel, but it also depended on the solid concentration (Takahashi, 2014). The relatively low flow velocity of the coarse-grained flow potentially caused by the increase in flow weight in which the denser the consolidation, the slower the flow velocity (Takahashi, 2014). This indicates that denser particles may lead to a rise in frictional resistance and reduce the flow velocity while proceeding downslope.

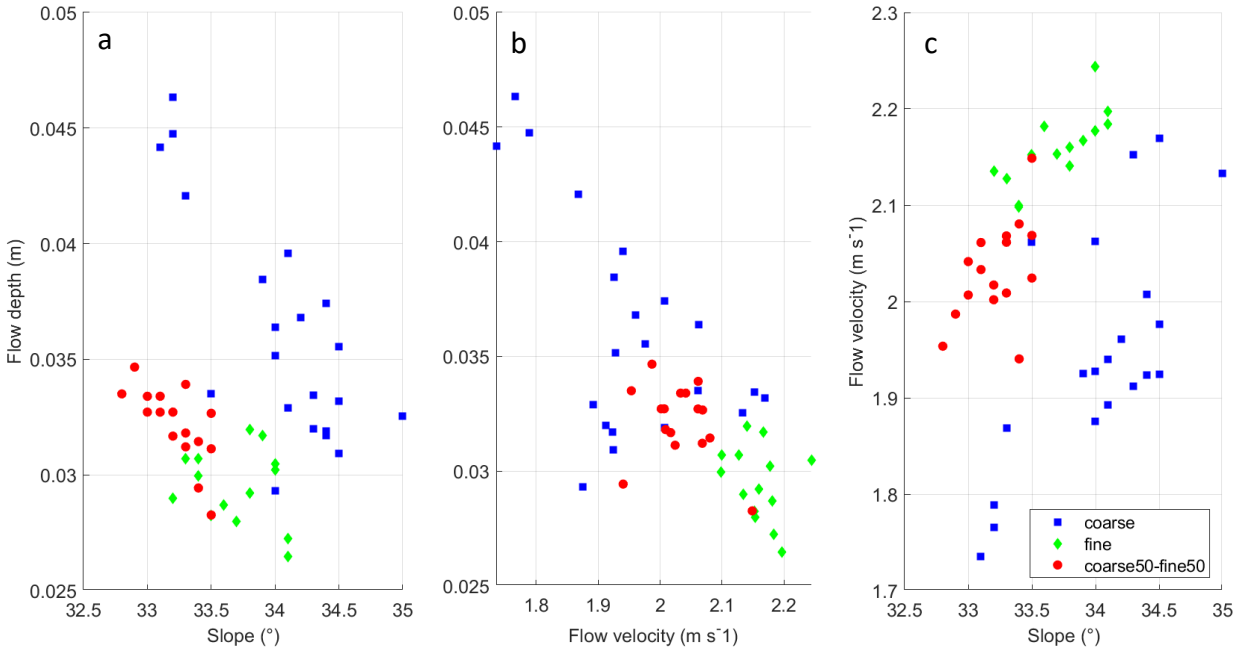

Figure 4.2 The relationship between flow depth and (a) Slope; (b) Flow velocity; (c) The relationship between flow velocity and slope.

4.2 Impact forces in dry granular flows

4.2.1 Quantification of impact forces using a geophone and load cell

The magnitude of particle impacts on the bed from the geophone was converted into amplitude in vertical and horizontal orientations. The comparison between geophone amplitude vertical and horizontal (*Figure 4.3*) resulted in relatively strong statistic (R^2 from 0.41 to 0.73) with relatively low p-value (<0.05) for all flow compositions. This indicates that both amplitudes were reliable enough to represent the impact forces, despite the value of geophone amplitude vertical being higher than the horizontal. Therefore, in this study, the geophone amplitude vertical was used for further analysis. Both amplitudes increased with increasing grain-size, wherein the coarse-grained flow was the highest. It is apparent that the coarser particle had a higher flow weight and generated a higher impact on the bed.

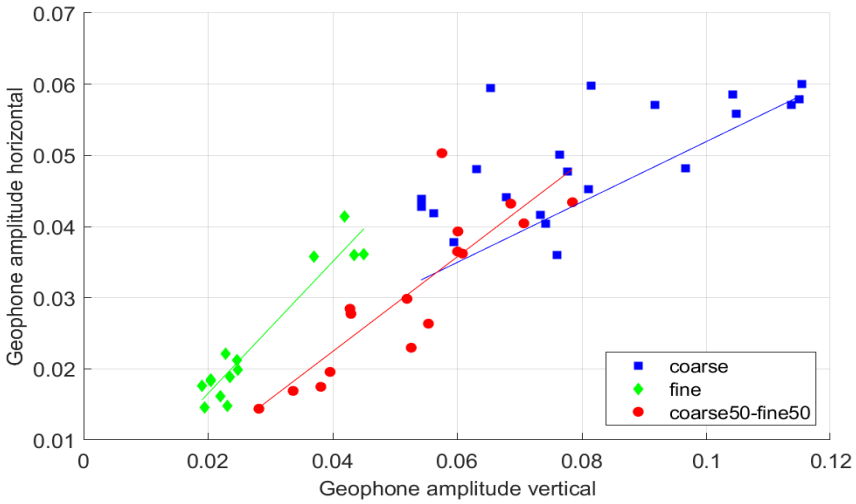

Figure 4.3 The comparison between geophone amplitude vertical and horizontal.

The behaviour of geophone and load cell were similar both in seismic wave and amplitude (*Figure 4.4*). Both amplitudes were able to simulate the particle impact and bed pressure fluctuation during the flow movement downslope, in which the highest amplitude occurred at the flow front, while the lower amplitude emerged at the flow body and tail. Multiple minor amplitudes appeared at the tail, probably from the jumping particles. Both amplitudes increased with increasing grain-size, wherein the coarse-grained flow was the highest, while the fine-grained flow was the lowest. Moreover, the comparison between the geophone amplitude vertical and the weight noise amplitude (*Figure 4.5*) resulted in relatively strong statistic (R^2 = 0.63) with relatively low p-value (<0.05) and implies a significant similarity between geophone and load cell.

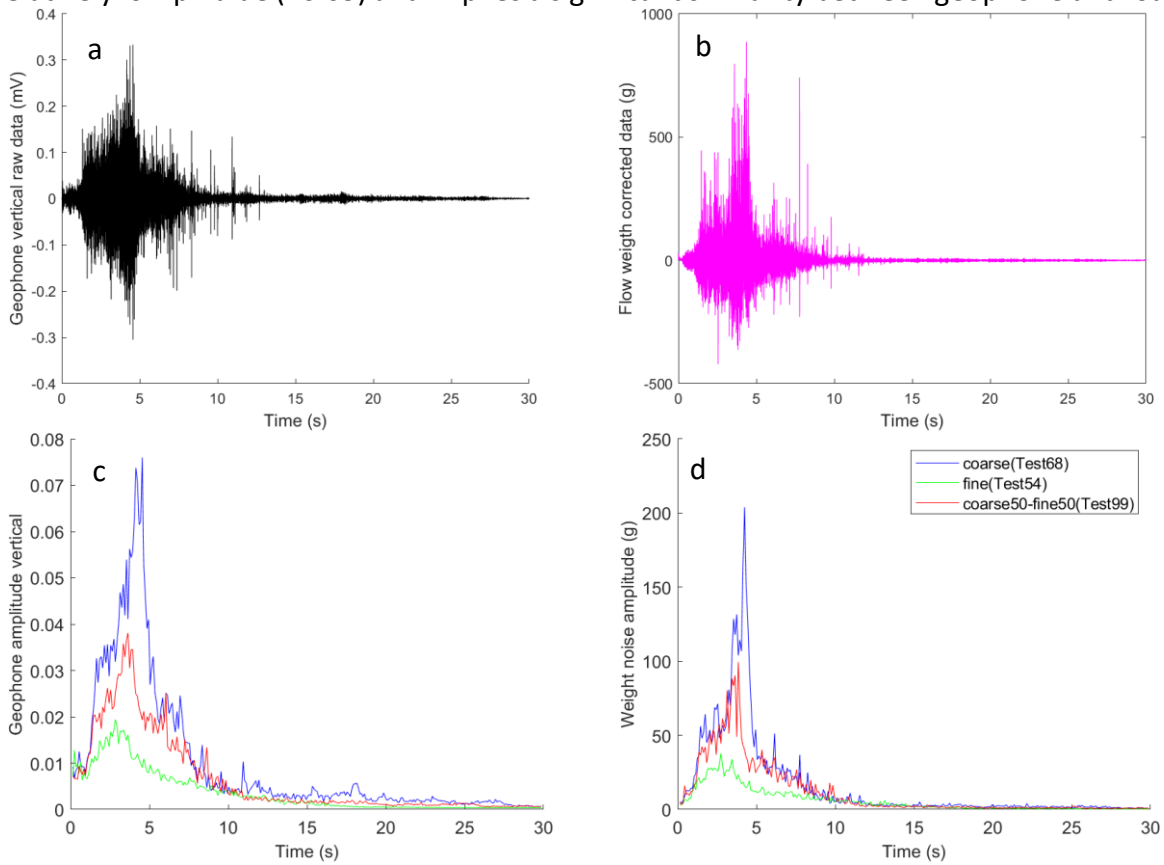

Figure 4.4 (a) The raw signal of geophone amplitude vertical; (b) The corrected data of flow weight. The comparison of three flows: (c) Geophone amplitude vertical; (d) Weight noise amplitude.

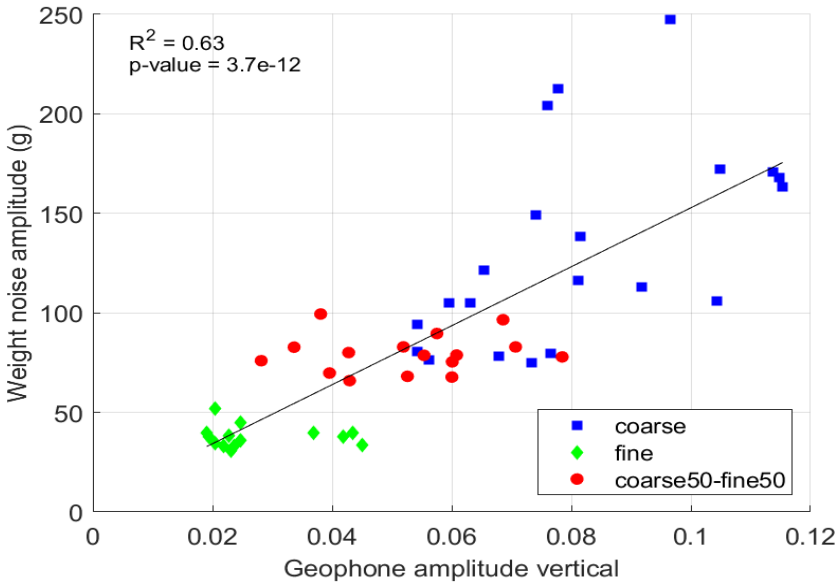

Figure 4.5 The comparison between geophone amplitude vertical and weight noise amplitude.

4.2.2 Flow controls impact forces

Geophone amplitude vertical increased with increasing grain-size at the same slope (*Figure 4.6a*). A similar trend also occurred at the same flow depth, flow velocity, and basal-shear forces (*Figure 4.6b, c, d*). The highest amplitude tended to occur in the coarse-grained flow, while a lower amplitude emerged in the finer-grained flow. This was perhaps because the fine-grained flow had less weight and generated a lower magnitude. Despite the high variability of the experimental data, in general, geophone amplitude vertical increased with increasing flow depth and basal-shear forces but decreased with the increasing flow velocity.

The natural variability in dry granular flows dynamic, the highly variable and stochastic nature of the bed entrainment mechanism and the limited experimental data for a different flow composition may result in relatively weak statistics with relatively high p-values. Nevertheless, all of the correlation between geophone amplitude vertical and the variables (i.e. slope, flow depth, flow velocity, basal-shear forces) indicated that the coarse-grained flow resulted in the highest amplitude. This is likely because of the larger grain-size correlated to a higher flow depth and heavier flow weight, which developed a more significant gravel fraction, which may correlate to the increase in impact forces (Haas and Woerkom, 2016).

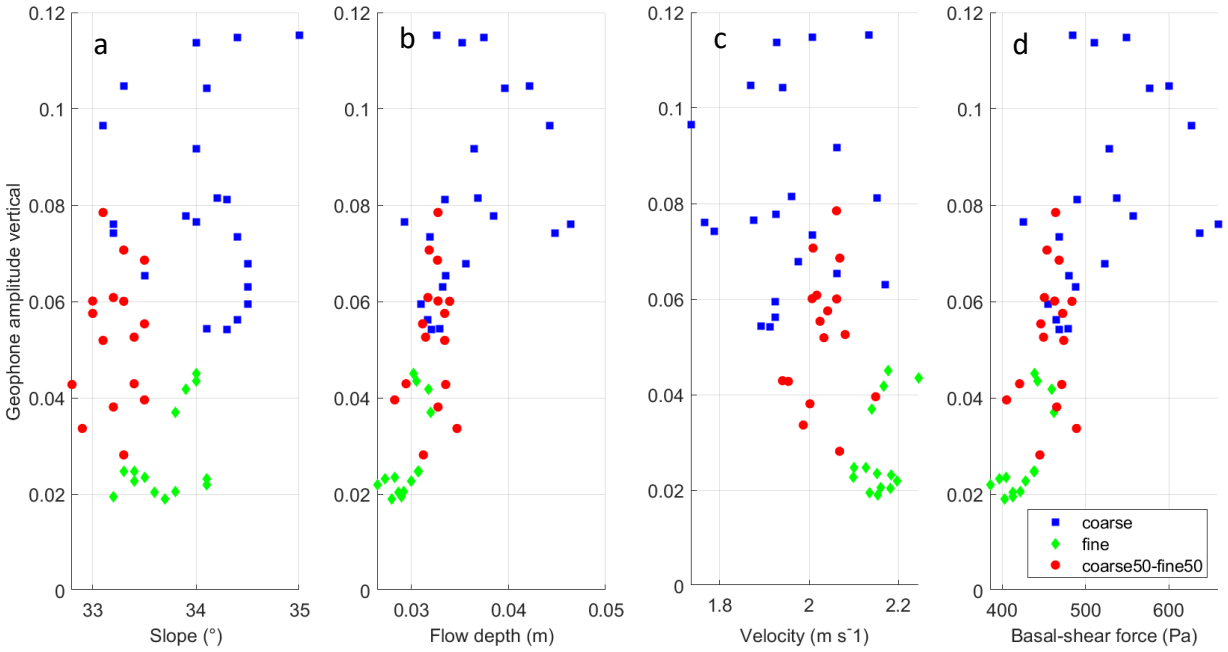

Figure 4.6 The relationship between geophone amplitude vertical and (a) Slope; (b) Flow depth; (c) Flow velocity; (d) Basal-shear forces.

4.3 Erosional mechanism

The experimental dry granular flows demonstrated that debris-flow erosion generally occurs by progressive scour rather than a mass failure of bed material (*Figure 4.7*). The erosion in a different flow composition can be seen in *Figure 4.9*. The erosional mechanism begins when the debris flows came down the channel flume by the interaction between the flow particles and the bed particles (*Figure 4.7b*). In this phase, as soon as the debris-avalanche material encountered the bed material, the entraining or incorporating of bed sediments grain by grain began to dominate the erosional mechanism by eroding the bed and generating a plowing bed as stated by Lu et al. (2016). This may correspond to a thin layer of the flow front, in which particle collision was more significant. Thus, the upper part of the bed became unstable due to repeated agitation and gravity force, then localised failures of upper parts of the bed occurred (*Figure 4.7c*). Once again, the failed parts of the bed blended with the flow and moved downstream due to basal abrasion, which occurs when the avalanche materials slide parallel to the bed material (Lu et al., 2016). Once the debris flow stopped, the flow consolidated and was deposited downstream. Larger materials dominated the surface of the flow and also centred in the middle part of the flow (*Figure 4.7d*).

Figure 4.7 The erosional mechanism: (a) Before experiment; (b) The initiation phase; (c) The motion phase; (d) The deposition phase; The flow travel time is 30 seconds for each experiment.

It appeared that bed entrainment by entraining or incorporating bed sediments grain by grain was probably more dominant than en masse failure of parts of the bed. In general, erosion in the coarse-grained flow was higher than in the finer-grained flow. Progressive scour from grain by grain interaction was confirmed by high erosion in the coarse-grained flow (*Figure 4.8*). The same trend also occurred in relation to flow depth, which proved the linear correlation between flow depth (*Figure 4.8b*) and basal-shear forces (*Figure 4.8d*) as shown in Equation (3) wherein the coarse-grained flow resulted in the highest erosion, despite having a similar flow depth and basal-shear forces.

Meanwhile, mass failure of bed material likely depended on the correlation between slope and erosion wherein erosion increased with channel slope both in coarse-grained flow or finer-grained flow, despite a few samples in the mixed flow showing an opposite trend and relatively scattered data in the coarse-grained flow (*Figure 4.8a*). At the same slope, erosion was relatively higher in the mixed flow, but at the steeper slope, erosion in the fine-grained flow was higher than the mixed flow. Despite a steeper slope generally resulting in higher flow velocity due to gravitational force and linearly increased the flow depth, flow composition was also important. A steeper slope in the coarse-grained flow produced low flow velocity with high flow depth and erosion. It indicated flow composition was possibly more significant than flow properties (i.e. flow depth, flow velocity) and channel slope in entraining bed material.

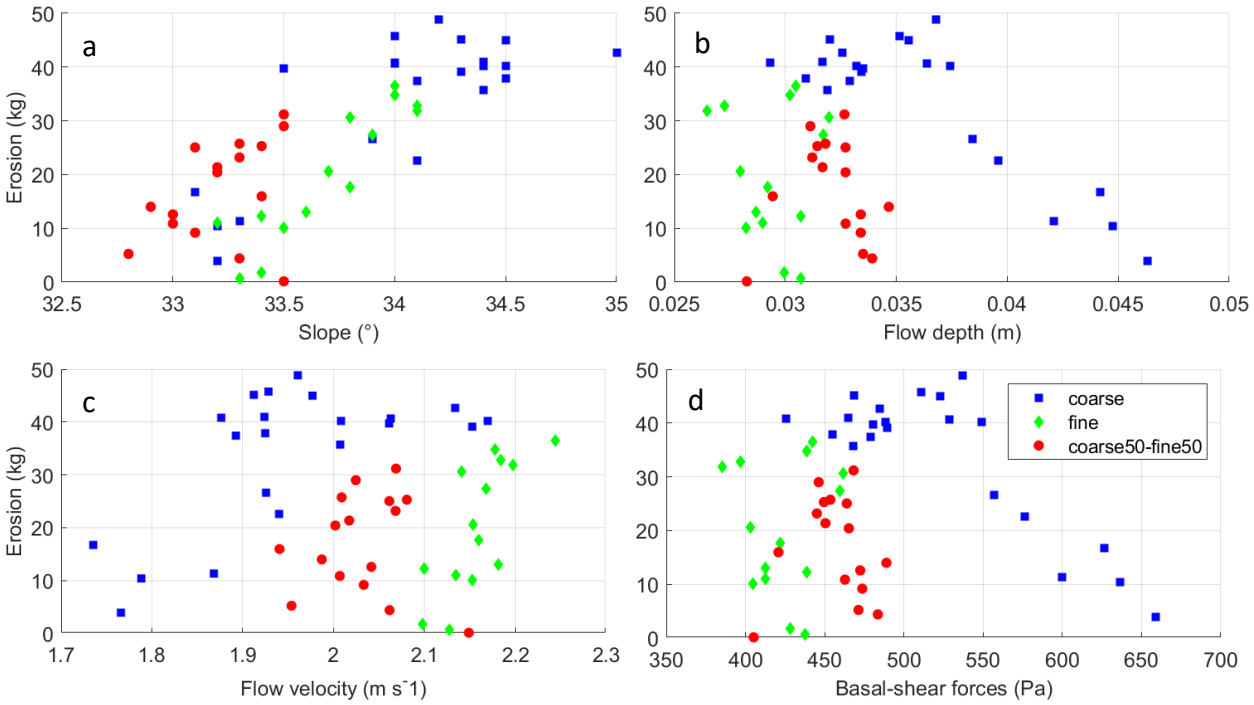

Figure 4.8 The relationship between erosion and (a) Slope; (b) Flow depth; (c) Flow velocity; (d) Basal-shear forces.

Figure 4.9 The erosion in a different flow composition: (a) Before experiments; (b) Coarse-grained flow (Test68); (c) Fine-grained flow (Test54); (d) Mixed flow (Test99).

5. DISCUSSION

5.1 The utilisation of geophone and load cell in quantifying impact forces

This study supports the use of geophone and load cell on a laboratory-scale to quantify impact forces and flow weight of debris flows. Both sensors worked adequately, the geophone was able to quantify the magnitude of particle impacts on the bed directly, and the load cell was able to measure the bed pressure fluctuations and convert them into flow weight.

The amplitude generated from the geophone showed a linear relationship with the particle impacts on the bed, and the weight noise amplitude generated from the load cell also showed a linear relationship with the bed pressure fluctuations on the bed. In addition, both amplitudes were able to perform asymptotic configuration of debris flows with one major surge (*Figure 4.4c, d*). The shape of the geophone amplitude indicated the fluctuating impact forces, and the weight noise amplitude demonstrated the fluctuating flow weight, during the flow movement downslope. It confirms that geophone is capable of quantifying impact forces, and the load cell is capable of measuring flow weight on the laboratory-scale.

The geophone amplitude shape showed consistency with the three phases of impact forces stated by Cui et al. (2015): 1) high value of impact forces which is a sudden strong impact at the flow front occurring when the peak amplitude shape emerged; 2) lower impact forces at the flow body occurring when the continuous amplitude shape emerged; and 3) low impact forces at the tail occurred when the slightly static amplitude shape emerged. A few minor peak amplitudes appeared at the tail, apparently due to jumping particles at the bed. The weight noise amplitude showed a linear relationship with the geophone amplitude, in which high amplitude indicated a large flow weight as well as high impact forces. This means that both sensors were capable of reproducing natural field-scale debris flows events.

The geophone neglected a channel slope correction due to a dynamic movement of the sensor which followed the flume inclination during the experiments. It possibly performed a more accurate measurement due to less calibration or correction. Additionally, both amplitudes were capable of determining a clear trend of impact forces and flow weight in debris flows of different composition wherein the amplitude increased with increasing grain-size. The highest amplitude was produced in the coarse-grained flow, while the lower amplitude was produced in the finer-grained flow. This implies that both sensors were able to characterize the debris flow composition.

5.2 The relative importance of impact forces in debris flows of different composition

Despite high variability in the experimental data, this study showed that the particles interacted with collisional and frictional contacts with the bed during its motion downslope, classified as the intermediate dry granular flows regime as discussed by Jiang et al. (2015). The collisional contacts resulted in impact forces, while the frictional contacts resulted in basal-shear forces. Nevertheless, it is possible that the impact forces became more significant because the collisional regime developed in the shallow layer of a dry granular flow, in which the upper part of the flow was more dominant rather than the frictional regime developed in the deeper layer. It was shown by the mass movement during the experiments (*Figure 4.7c*), which collisional contacts drove more particles downslope.

In general, impact forces were highest in the coarse-grained flow, and lower when the grain-size decreased, and the lowest impact forces were found in the fine-grained flow, while intermediate

impact forces were found in the mixed flow. Impact forces increased with increasing flow depth and flow weight, but decreased with the increasing flow velocity. At the same slope, impact forces were also highest in the coarse-grained flow compared to other flows. It was found that the coarse-grained flow resulted in the highest flow depth and flow weight, but resulted in the lowest flow velocity. This indicates that debris flow composition mainly affects the flow dynamics (i.e. flow depth, flow velocity, flow weight) which consistent with the results from flume experiment by Haas and Woerkom (2016).

Despite flow velocity showing an opposite trend in which impact force decreased with increasing flow velocity, it suggested that the gravel fraction during the mass movement was more dominant in increasing impact forces than the channel slope. It implies that larger grain-size connected to an increasing flow depth and flow weight, which produced a more significant gravel fraction, may relate to an increase in impact forces as suggested by Haas and Woerkom (2016). In addition, it also indicated that impact forces increased with increasing flow depth, notably in the coarser grains, as stated by Cui et al. (2015).

This evidence suggests that impact forces were more significantly driven by debris flow composition. (i.e. grain-size distribution) and moderately by flow properties (i.e. flow depth, flow weight, flow velocity) as stated by Cui et al. (2015) and Hubl et al. (2009) wherein the variance of impact forces depends on the distributions of the grain in the flow (which refers to the debris flow composition).

5.3 Erosion dependence on debris flow composition

The energy of sliding masses is transmitted to the bed material during the mass movement by the interaction between the particles of the flow and the particles at the bed. The particles created potential energy, then kinetic energy when it started to flow. The impact forces and basal-shear forces act during this mass transfer process, then together with flow velocity generate flow momentum, thus causing bed entrainment. The different debris flow compositions and masses may result in a different amount of energy and therefore have a different bed entrainment mechanism.

This study suggests that the bed entrainment by incorporation of bed sediments grain by grain is possibly more dominant than en masse failure of parts of the bed. This may be due to more significant collisional contacts rather than frictional contacts between the particles at the flow and the particles at the bed, in which collisional contacts relate to the impact forces and frictional contacts relate to the basal-shear forces. It implies that the impact forces are more critical in affecting the debris-flow erosion, mainly by progressive scour mechanism rather than mass failure due to a sudden interaction between the flow particles with the bed material.

In general, there is a slight trend between erosion and flow properties (i.e. flow depth, flow velocity) and channel slope in which erosion increased with increasing flow properties and channel slope. Nevertheless, erosion showed correlation to grain-size; erosion was highest in the coarse-grained flow and lowered in the finer-grained flow as discussed by Haas and Woerkom (2016). This suggests that debris flow composition (i.e. grain-size distribution) exerted stronger control over bed entrainment than flow properties (i.e. flow depth, flow velocity) and channel slope and the debris flow composition mainly affected the flow dynamics (i.e. flow depth, flow velocity), thus also potentially enhancing the erosive potential as stated by De Haas et al. (2015). It is also similar to the study by Hsu et al. (2008) which indicated a strong dependence of erosion on particle diameter (e.g. debris flow composition).

Erosion increased with increasing grain-size and impact forces also increased with increasing grain-size. Both erosion and impact forces were significantly controlled by the debris flow composition (i.e. grain-size distribution), indicating that erosion increased when gravel fraction increased. This may relate to the increase in impact forces enhancing the total forces at the bed, and thus, also erosion as explained by Haas and Woerkom (2016). This suggests that impact forces significantly affected debris-flow erosion, wherein erosion increased with increasing impact forces.

5.4 Recommendation

In this study, the impact forces were also calculated by using Equation (1); however, the result showed a less significant compared to the basal-shear forces calculated by using Equation (3); thus, it was not used for further analysis. The less significant value was likely due to the calculation only using a single value of flow velocity; flow velocity at the flow front and the flow body or the tail may be different during its travel downslope. Besides, there was a constant value of impact forces from the geophone amplitude found in the fine-grained flow even though the other variables (i.e. slope, flow depth, flow velocity, erosion) changed. In addition, the study was limited to dry granular flows, which only covered the solid fraction with one type of material (i.e. gravel). Several experiments for each type of dry granular flows were not performed at a similar channel slope, which may lead to scattered results and weak correlation.

Future work should include a wider variety of debris flow composition that represents the solid and fluid fractions as classified by Takahashi (2014) (i.e. the stony-type, the turbulent-muddy-type, and the viscous-type) and at a similar channel slope to achieve better correlation. The implementation of geophone on the laboratory-scale also can be improved to quantify the flow velocity, which may provide a more significant calculation of impact forces. In addition, a laser scanner can be installed above the channel flume to observe the spatial pattern of particle distribution during its movement. Better optical measurements and video observations can probably be achieved if the flume side were made from glass.

6. CONCLUSION

In this study, the relative importance of impact forces in debris flows of different composition was investigated by quantifying impact forces and unravelling how impact forces affect debris-flow erosion. During this study, a total of 104 experiments were done with three different compositions for the flow (i.e. coarse-grained flow, fine-grained flow, mixture flow of coarse-grained and fine-grained) and two different compositions for the bed material (i.e. coarse-grained bed, fine-grained bed). The experiment used a larger dimension of channel flume and implemented measurement devices (i.e. geophone, load cell, laser distance measuring instrument) based on flume experiment by Haas and Woerkem (2016).

Fifty-nine samples were resulting in erosion, while 45 samples resulted in a deposition during the experiment. The impact forces represented by the geophone amplitude were compared with the weight noise amplitude to examine the capability of geophone in quantifying impact forces and load cell in measuring flow weight on the laboratory-scale. Thus, a comparison between the flow properties (i.e. flow depth, flow velocity), slope, and basal-shear forces is necessary to investigate which variable is more significant to impact forces.

From this study, three main conclusions can be established: (1) the geophone is capable of quantifying impact forces and load cell capable of measuring flow weight on the laboratory-scale. Despite using dry granular flows, both sensors were able to reproduce natural field-scale debris flows events and characterise debris flow composition; (2) impact forces were more significantly driven by debris flow composition (i.e. grain-size distribution) and moderately by flow properties (i.e. flow depth, flow weight, flow velocity) wherein the variance of impact forces depends on the distribution of the grain in the flow (i.e. debris flow composition); (3) debris flow composition (i.e. grain-size distribution) strongly controlled the bed entrainment mechanism rather than flow properties (i.e. flow depth, flow velocity) and channel slope. In addition, impact forces significantly affected debris-flow erosion, mainly by the progressive scour mechanism rather than mass failure, wherein erosion increased with increasing impact forces.

Dry granular flows may able to represent debris flows, particularly in bed entrainment driven by impact forces. The flume experiments were capable of reproducing debris flows similar to natural field-scale debris flows events, while the measurement devices were capable of quantifying impact forces and unravelling how impact forces affect debris-flow erosion. It was suggested that debris flow composition has a vital role in driving impact forces rather than the flow properties (i.e. flow depth, flow weight, flow velocity), thus affecting the erosive potential.

Although this study was able to quantify impact forces in debris flows of a different composition and unravel how impact forces affect debris-flow erosion with a dry granular flow experiments and implementation of measurement devices (i.e. geophone, load cell, laser distance measuring instrument), future research should be performed using a wider variety of debris flow compositions, further utilisation of geophone or other measurement devices on the laboratory-scale, and a further development of debris flow flumes.

ACKNOWLEDGEMENT

This work was supported by the Netherlands Organization for Scientific Research (NWO) (grant to Tjalling de Haas) and the Indonesia Endowment Fund for Education or *LPDP* (master programme scholarship to Ika Prinadiastari). This work is part of the MSc thesis project of IP. We gratefully acknowledge technical support by Arjan van Eijk, Bas van Dam, Henk Markies and Marcel van Maarseveen.

REFERENCES

Arattano, M., Franzi, L. (2003). On the evaluation of debris flows dynamics by means of mathematical models. *Natural Hazards and Earth System Sciences 3(6)*, 539–544.

Armanini, A. (1997). On the dynamic impact of debris flows. *Lecture Notes in Earth Sciences. In Recent Development on Debris Flows, Armanini A, Michiue M (eds)*, *64*, 208–226. Springer: Berlin.

Armanini, A., Dalrì, C., Putta F.D., Larcher, M., Rampanelli, L., Righetti, M. (2004). Experimental Analysis on the Hydraulic Efficiency of Mudflow Breakers. *In Proceedings of the International Conference on Hydraulics of Dams and River Structures, Yazdandoost F, Attari J (eds)*. Taylor & Francis Group: London.

Bagnold, R.A. (1954). Experiments on a gravity-free dispersion of large solid spheres in a Newtonian fluid under shear: *Proceedings of the Royal Society of London*, *Ser. A 225*, 49–63.

Berger, C., McArdell, B. W., & Schlunegger, F. (2011). Direct measurement of channel erosion by debris flows, Illgraben, Switzerland. *Journal of Geophysical Research: Earth Surface*, *116*(1), 1–18. https://doi.org/10.1029/2010JF001722

Beverage, J.P., and J. K. Culbertson. (1964). Hyper-concentrations of suspended sediment. *J. Hydraul. Div. Am. Soc. Civ. Eng., 90(HY6)*, 117-128.

Coe, J. A., Kinner, D. A., & Godt, J. W. (2008). Initiation conditions for debris flows generated by runoff at Chalk Cliffs, central Colorado. *Geomorphology*, *96*(3–4), 270–297. https://doi.org/10.1016/j.geomorph.2007.03.017

Cui, P., Zeng, C., & Lei, Y. (2015). Experimental analysis on the impact force of viscous debris flow. *Earth Surface Processes and Landforms*, *40*(12), 1644–1655. https://doi.org/10.1002/esp.3744

De Haas, T., Braat, L., Leuven, J. R. F. W., Lokhorst, I. R., & Kleinhans, M. G. (2015). Effects of debris flow composition on runout, depositional mechanisms, and deposit morphology in laboratory experiments. *Journal of Geophysical Research F: Earth Surface*, *120*(9), 1949–1972. https://doi.org/10.1002/2015JF003525

Egashira, S., Itoh, T., and Takeuchi, H. (2001). Transition Mechanism of Debris Flow over Rigid Bed to Erodible Bed. *J. Phys. and Chem. Earth B 26(2)*, 169–174.

Haas, T. de, & Woerkom, T. van. (2016). Bed scour by debris flows: experimental investigation of effects of debris-flow composition. *Earth Surface Processes and Landforms*, *41*(13), 1951–1966. https://doi.org/10.1002/esp.3963

Hübl, J., Suda, J., Proske, D., Kaitna, R., Scheidl C. (2009). Debris Flow Impact Estimation. Ohrid: Macedonia.

Huang, H.P., Yang, K.C., Lai, S.W. (2007). Impact force of debris flow on filter dam. *Geophysical Research Abstracts. European Geosciences Union-General Assembly*. Vienna, Austria, 03218.

Hsu, L., Dietrich, W. E., & Sklar, L. S. (2014). Mean and fluctuating basal forces generated by granular flows: Laboratory observations in a large vertically rotating drum. *Journal of Geophysical Research: Earth Surface*, *119*(6), 1283–1309. https://doi.org/10.1002/2013JF003078

Hsu, Leslie, Dietrich, W. E., & Sklar, L. S. (2008). Experimental study of bedrock erosion by granular flows. *Journal of Geophysical Research: Earth Surface*, *113*(2). https://doi.org/10.1029/2007JF000778

Iverson, R. M. (1997). of Debris. *Review of Geophysics*, *35*(97), 245–296.

Iverson, R. M., Reid, M. E., Logan, M., LaHusen, R. G., Godt, J. W., & Griswold, J. P. (2011). Positive feedback and momentum growth during debris-flow entrainment of wet bed sediment. *Nature Geoscience*, *4*(2), 116–121. https://doi.org/10.1038/ngeo1040

Iverson, R.M., and Vallance, J.W. (2001). New views of granular mass flows: *Geology, 29*, 115–118. https://doi: 10.1130/0091- 7613(2001)029<0115:NVOGMF>2.0.CO;2.

Jiang, Y. J., Zhao, Y., Towhata, I., and Liu, D. X. (2015). Influence of particle characteristics on impact event of dry granular flow. *Powder Technology*, *270*(Part A), 53–67. https://doi.org/10.1016/j.powtec.2014.10.005

Johnson, A.M. (1984). Debris flow, in Slope Instability. *Edited by D. Brunsden and D. B. Prior*, 257-361. John Wiley, New York.

Kaitna, R, Dietrich, W., Hsu, L. (2014). Surface slopes, velocity profiles and fluid pressure in coarse-grained debris flows saturated with water and mud. *Journal of Fluid Mechanics 741*, 377–403.

Kean, J. W., McCoy, S. W., Tucker, G. E., Staley, D. M., & Coe, J. A. (2013). Runoff-generated debris flows: Observations and modeling of surge initiation, magnitude, and frequency. *Journal of Geophysical Research: Earth Surface*, *118*(4), 2190–2207. https://doi.org/10.1002/jgrf.20148

Krein, A., Klinck, H., Eiden, M., Symader, W., Bierl, R., Hoffmann, L., Pfister, L. (2008). Investigating the transport dynamics and the properties of bedload material with a hydroacoustic measuring system. *Earth Surface Processes and Landforms 33*, 152–163.

Lu, P. yuan, Yang, X. guo, Xu, F. gang, Hou, T. xing, & Zhou, J. wen. (2016). An analysis of the entrainment effect of dry debris avalanches on loose bed materials. *SpringerPlus*, *5*(1), 1–15. https://doi.org/10.1186/s40064-016-3272-4

Major, J. J., & Iverson, R. M. (1999). Debris-flow deposition: Effects of pore-fluid pressure and friction concentrated at flow margins. *Bulletin of the Geological Society of America*, *111*(10), 1424–1434. https://doi.org/10.1130/0016-7606(1999)111<1424:DFDEOP>2.3.CO;2

McArdell, B. W., Bartelt, P., & Kowalski, J. (2007). Field observations of basal forces and fluid pore pressure in a debris flow. *Geophysical Research Letters*, *34*(7), 2–5. https://doi.org/10.1029/2006GL029183

Mitchell, J. K. (1976). Fundamentals of Soil Behavior, *422*. John Wiley, New York.

Mizuyama, T, Laronne, J.B., Nonaka, M., Sawada, T., Satofuka, Y., Matsuoka, M., Yamashita, S., Sako, Y., Tamaki, S., Watari, M., Yamaguchi, S., Tsuruta. K. (2010a). Calibration of a passive acoustic bedload monitoring system in Japanese mountain rivers. *In Bedload-surrogate Monitoring Technologies, Gray JR, Laronne JB, Marr JDG (eds), US Geological Survey Scientific Investigations Report 2010–5091. US Geological Survey: Reston, VA*, 296–318. http://pubs.usgs.gov/sir/2010/5091/papers/listofpapers.html [accessed on 24 November 2010]

Moriguchi, S., Borja, R. I., Yashima, A., and Sawada, K. (2009). Estimating the impact force generated by granular flow on a rigid obstruction. *Acta Geotechnica*, *4*(1), 57–71. https://doi.org/10.1007/s11440-009-0084-5

Ogawa, S. (1978). Multi-temperature theory of granular materials, in Cowin, S.C., and Satake, M., eds. *Proceedings of the US-Japan Seminar on Continuum-Mechanical and Statistical Approaches in the Mechanics of Granular Materials, Tokyo: Tokyo, Gakujutsu Bunken Fukyukai*, 207–217.

Pierson T.C., Janda R.J., Thouret J.C. & Borrero C.A. (1990). Perturbation and melting of snow and ice by the 13 November 1985 eruption of Nevado del Ruiz, Columbia and consequent mobilization, flow and deposition of lahars. *Journal of Volcanology and Geothermal Research, 41*, 17-66.

Pierson, T. C., and J. E. Costa. (1987). Archeologic classification of subaerial sediment-water flows, in Debris Flows/Avalanches: *Process, Recognition, and Mitigation, Rev. Eng. Geol., vol. 7, edited by J. E. Costa and G. F. Wieczorek*, 1-12. Geol. Soc. of Am., Boulder, Colo.

Reid, M. E., Iverson, R. M., Logan, M., Lahusen, R. G., Godt, J. W., & Griswold, J. P. (2011). Entrainment of bed sediment by debris flows: Results from large-scale experiments. *International Conference on Debris-Flow Hazards Mitigation: Mechanics, Prediction, and Assessment, Proceedings*, 367–374. https://doi.org/10.4408/IJEGE.2011-03.B-042

Rickenmann, D., Turowski, J. M., Fritschi, B., Klaiber, A., & Ludwig, A. (2012). Bedload transport measurements at the Erlenbach stream with geophones and automated basket samplers. *Earth Surface Processes and Landforms*, *37*(9), 1000–1011. https://doi.org/10.1002/esp.3225

Rickenmann, D., Turowski, J. M., Fritschi, B., Wyss, C., Laronne, J., Barzilai, R., … Habersack, H. (2014). Bedload transport measurements with impact plate geophones: Comparison of sensor calibration in different gravel-bed streams. *Earth Surface Processes and Landforms*, *39*(7), 928–942. https://doi.org/10.1002/esp.3499

Savage, S.B. (1984). The mechanics of rapid granular flows. *Adv Appl Mech 24*, 289–366

Sharp, R. P., and L. H. Nobles. (1953). Mudflow of 1941 at Wrightwood, southern California. *Geol. Soc. Am. Bull., 64*, 547–560. https://doi:10.1130/ 0016-7606(1953)64.

Sitar, N., S. A. Anderson, and K. A. Johnson. (1992). Conditions for initiation of rainfall-induced debris flows, *in Stability and Performance of Slopes and Embankments II Proceedings*, 834-849. Geotech. Eng. Div., Am. Soc. of Civ. Eng., New York.

Stock, J. D., & Dietrich, W. E. (2006). Erosion of steepland valleys by debris flows. *Bulletin of the Geological Society of America*, *118*(9–10), 1125–1148. https://doi.org/10.1130/B25902.1

Takahashi, T. (1991). Debris Flow. *IAHR Monograph Series, Balkema, Rotterdam, The Netherlands*, 165.

Takahashi, T. (1981). Debris flow. In *Annual review of fluid mechanics, volume 13*.

Takahashi, T. (2014). Debris flow: mechanics, prediction and countermeasures. CRC press.

Takahasi, K. (1937). On the dynamical properties of granular mass. *Geophys Mag 11*, 165–175

Theule, J. I., Liébault, F., Laigle, D., Loye, A., & Jaboyedoff, M. (2015). Channel scour and fill by debris flows and bedload transport. *Geomorphology*, *243*, 92–105. https://doi.org/10.1016/j.geomorph.2015.05.003

Varnes, D. J. (1978). Slope movement types and processes, *in Land- slides--Analysis and Control, edited by R. L. Schuster and R. J. Krizek, Spec. Rep. Natl. Res. Counc. Transp. Res. Board, 176*, 11-33. Natl. Acad. of Sci., Washington, D.C.

Wyss, C. R., Rickenmann, D., Fritschi, B., Turowski, J. M., Weitbrecht, V., & Boes, R. M. (2016). Measuring bed load transport rates by grain-size fraction using the swiss plate geophone signal at the erlenbach. *Journal of Hydraulic Engineering*, *142*(5). https://doi.org/10.1061/(ASCE)HY.1943-7900.0001090

Yamagishi, M., Mizuyama, T., Satofuka, Y., and Mizuno, H. (2003). Behavior of Big Boulders in Debris Flow Containings and Gravel. *In: Rickenmann, D. and Chen,C. (eds), Proceedings oftheASCEInternational Conference on Debris-Flow Hazards Mitigation: Mechanics, Prediction & Assessment, Davos, Switzerland*, 411–420.

Yohannes, B., Hsu, L., Dietrich, W. E., & Hill, K. M. (2012). Boundary stresses due to impacts from dry granular flows. *Journal of Geophysical Research: Earth Surface*, *117*(2), 1–21. https://doi.org/10.1029/2011JF002150

Zanuttigh, B., Lamberti, A. (2006). Experimental analysis of the impact of dry avalanches on structures and implication for debris flows. *Journal of Hydraulic Research 44(4)*, 522–534.

SUPPLEMENTARY MATERIAL

File `Experimental Data of Erosion ´: File (Table 1.xlsx) containing experimental data of each debris flow resulted in erosion

Folder `Photos & Videos of Erosion ´: Folder containing photos and videos taken after each debris flow resulted in erosion